

Experimental Demonstration of the Effect of the Number of Qubits Against CPU Processing Time on Quantum Hadamard Edge Detection (QHED)

Desi Amirullah and Lipantri Mashur Gultom
Politeknik Negeri Bengkalis, Indonesia

Keywords: Quantum, Hadamard, Qubit, Edge Detection.

Abstract: This study focuses on the Quantum Hadamard Edge Detection (QHED) experiment in detecting the edges of an image where it is proven the effect of the number of qubits on CPU processing time. The image dataset being tested is contour detection and image segmentation resources from the Berkeley Computer Vision Group. the number of qubits that gave the final results of this study were 2, 4, 6, 8, 10 and 12 qubits, while those above 12 qubits were unable to be tested with the devices used in this study. the final result of the experiment proves that QHED can detect the edges of an image with the fastest processing time on the use of the number of qubits is 6 while the best edge detection process results are 2 qubits.

1 INTRODUCTION

Quantum Hadamard Edge Detection (QHED) is one of the edge detection algorithms with a quantum computing approach using hadamard transformation. QHED has an image encoding scheme that is efficient in saving memory space by using amplitude coding for an exponential decrease in the number of qubits used, namely $n = \log_2 N$ (Geng, 2022). However, the time complexity of initial preparation for image coding is very high. Therefore, this study focuses on analyzing how the number of qubits used in QHED affects the time and memory space used (Yan, 2016).

QHED uses the Hadamard gate (H) as a qubit transform operation (Yuan, 2019).

$$\begin{aligned} |0\rangle &= \frac{(|0\rangle + |1\rangle)}{\sqrt{2}} \\ |1\rangle &= \frac{(|0\rangle - |1\rangle)}{\sqrt{2}} \end{aligned} \quad (1)$$

then the N-pixel images that are processed will be numbered using the binary bit-string $|b_{n-1}b_{n-2}b_{n-3} \dots b_1b_0\rangle$ where $b_i \in \{0,1\}$. For two adjacent pixels, it can be written as a bit-string pair $|b_{n-1}b_{n-2} \dots b_10\rangle$ and $|b_{n-1}b_{n-2} \dots b_11\rangle$ where only the least significant bit (LSB) is different from both.

Each of the corresponding (normalized) pixel intensity values can be written as $c_{b_{n-1}b_{n-2} \dots b_10}$ and $c_{b_{n-1}b_{n-2} \dots b_11}$. Then writing the pixel value can be simplified into a decimal representation, namely c_i and c_{i+1} . Then the application of the H gate to the LSB in the quantum register space becomes the unitary result as follows.

$$I_{2^{n-1}} \otimes H_0 = \frac{1}{\sqrt{2}} \begin{bmatrix} 1 & 1 & 0 & 0 & \dots & 0 & 0 \\ 1 & -1 & 0 & 0 & \dots & 0 & 0 \\ 0 & 0 & 1 & 1 & \dots & 0 & 0 \\ 0 & 0 & 1 & -1 & \dots & 0 & 0 \\ \vdots & \vdots & \vdots & \vdots & \ddots & \vdots & \vdots \\ 0 & 0 & 0 & 0 & \dots & 1 & 1 \\ 0 & 0 & 0 & 0 & \dots & 1 & -1 \end{bmatrix} \quad (2)$$

where $I_{2^{n-1}}$ is a matrix $2^{n-1} \times 2^{n-1}$. The unitary result containing the image pixel value into the quantum register is encoded using Quantum Probability Image Encoding (QPIE) (Ruan, 2021), (Wang, 2021).

$$|Img\rangle = \sum_{i=0}^{N-1} c_i |i\rangle \quad (3)$$

$$(I_{2^{n-1}} \otimes H_0) \cdot \begin{bmatrix} c_0 \\ c_1 \\ c_2 \\ c_3 \\ \vdots \\ c_{N-2} \\ c_{N-1} \end{bmatrix} \rightarrow \frac{1}{\sqrt{2}} \begin{bmatrix} c_0 + c_1 \\ c_0 - c_1 \\ c_2 + c_3 \\ c_2 - c_3 \\ \vdots \\ c_{N-2} + c_{N-1} \\ c_{N-2} - c_{N-1} \end{bmatrix} \quad (4)$$

Here's a circuit drawing to extract all the edge information from the image (Cavalieri, 2020).

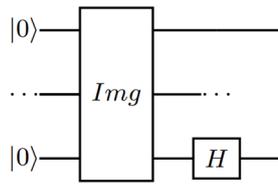


Figure 1: Circuit to get the differences $(c_0 - c_1), (c_2 - c_3)$.

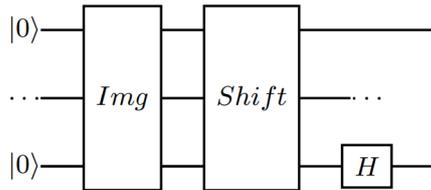


Figure 2: Circuit to get the differences $(c_1 - c_2), (c_3 - c_4)$.

From the results of the matrix equation (4), horizontal edge detection can be obtained between pairs of even number pixels: 0 & 1, 2 & 3, etc. and horizontal edge detection between pairs of odd number pixels: 1 & 2, 2 & 3, etc. So to obtain the value of the amplitude permutation in the quantum register by converting the amplitude vector $(c_0, c_1, c_2, \dots, c_{N-1})^T$ into $(c_1, c_2, c_3, \dots, c_{N-1})^T$. After that, it is transformed with an H gate and the quantum register measurements are carried out on the LSB until it becomes $|1\rangle$. In general, the following examples of image processing can be seen (Cavalieri, 2020).

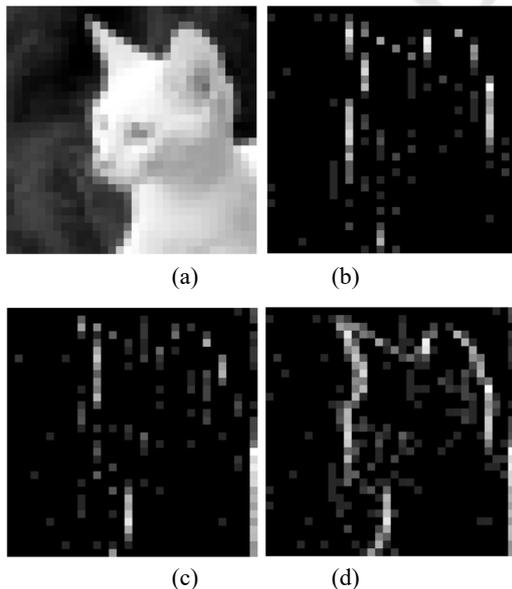


Figure 3: Example (a) image source, (b) image processing result from fig. 1, (c) image processing results from fig. 2 and (d) merging fig. 3, fig. 4 and fig. 5.

From research (yao, 2017) it can be varied with additional qubits to the quantum register so that it can expand the QHED algorithm in computing even and odd pixel pairs simultaneously. For example, from the previous step, initialize $|Img\rangle = (c_0, c_1, c_2, \dots, c_{N-1})^T$. Then the H gate is applied to additional qubits with initialization $|0\rangle$. In the end it produces a redundancy $(n + 1)$ qubits in the image represented by equation (5). Furthermore, the unity of the amplitude permutation is defined in equation (6) to change the amplitude into a structure that will facilitate the calculation of the image gradient value for the next stage.

$$|Img\rangle \otimes \frac{|0\rangle + |1\rangle}{\sqrt{2}} = \frac{1}{\sqrt{2}} \begin{bmatrix} c_0 \\ c_0 \\ c_1 \\ c_1 \\ c_2 \\ c_2 \\ \vdots \\ c_{N-2} \\ c_{N-2} \\ c_{N-1} \\ c_{N-1} \end{bmatrix} \quad (5)$$

$$D_{2^{n+1}} = \begin{bmatrix} 0 & 1 & 0 & 0 & \dots & 0 & 0 \\ 0 & 0 & 1 & 0 & \dots & 0 & 0 \\ 0 & 0 & 0 & 1 & \dots & 0 & 0 \\ 0 & 0 & 0 & 0 & \dots & 0 & 0 \\ \vdots & \vdots & \vdots & \vdots & \ddots & \vdots & \vdots \\ 0 & 0 & 0 & 0 & \dots & 0 & 1 \\ 1 & 0 & 0 & 0 & \dots & 0 & 0 \end{bmatrix} \quad (6)$$

Equation (6) is also known as the decrement gate (D) which can efficiently decompose the unitary result into a group of rotational gates, both single and multi-X controlled in the quantum register (Yao, 2017). More details can be seen in the following circuit picture.

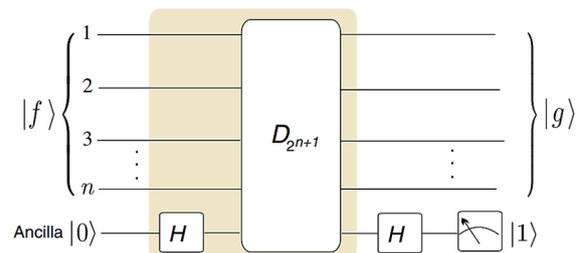


Figure 4: the QHED circuit with an auxiliary qubit.

By applying the gate $D_{2^{n+1}}$, will transform $(c_0, c_0, c_1, c_1, c_2, c_2, \dots, c_{N-2}, c_{N-2}, c_{N-1}, c_{N-1})^T$ into $(c_0, c_1, c_1, c_2, c_2, \dots, c_{N-2}, c_{N-1}, c_{N-1}, c_0)^T$. Then, by applying the H

gate to the additional qubits, we get a gradient for even and odd pixel pairs simultaneously.

$$(I_{2^n} \otimes H) \cdot \begin{bmatrix} c_0 \\ c_1 \\ c_1 \\ c_2 \\ c_2 \\ c_3 \\ \vdots \\ c_{N-2} \\ c_{N-1} \\ c_{N-1} \\ c_0 \end{bmatrix} \rightarrow \begin{bmatrix} c_0 + c_1 \\ c_0 - c_1 \\ c_1 + c_2 \\ c_1 - c_2 \\ c_2 + c_3 \\ c_2 - c_3 \\ \vdots \\ c_{N-2} + c_{N-1} \\ c_{N-2} - c_{N-1} \\ c_{N-1} + c_0 \\ c_{N-1} - c_0 \end{bmatrix} \quad (7)$$

measurement of this condition against additional qubits in the $|1\rangle$ measurement of this condition against additional qubits in the $c_i - c_{i+1}$ gradient for all possible values of the adjacent pair of qubits. Meanwhile, to get the edge detection value of the image vertically, you can use the transpose matrix of the image and then follow all the steps that have been described previously. For the final stage in producing the full edge detection method from this process, the results of processing horizontally and vertically must be combined.

2 EXPERIMENTAL PROCEDURES

This chapter focuses on the implementation of all the steps described in the previous chapter. while the image dataset tested used a benchmark dataset from contour detection and image segmentation resources from the Berkeley Computer Vision Group (Arbelaez, 2010). The program code is built using Qiskit and simulated with Qiskit backend state vector simulator. The hardware used is Dell Inspiron 3881 with 16 GB RAM memory (DDR4 SDRAM), Intel(R) Core(TM) i7-10700F CPU @ 2.90 GHz (8 Core) and Windows 10 Home Single Language 64 Bit Operating System.

The first step is preprocessing image data that will be processed into QHED (Pramanik, 2021).

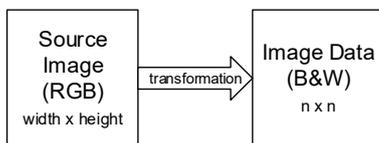


Figure 5: Preprocessing image data.

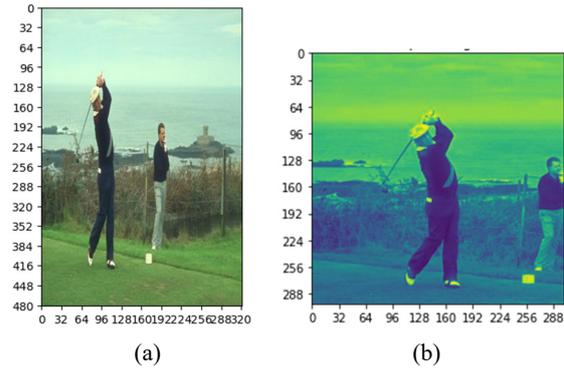


Figure 6: Example preprocessing image data : (a) RGB image with 481 x 321 pixel and (b) B&W image with 321 x 321 pixel.

Then, the number of qubits (N-qubits) and the chunk size of 2^{cp} re selected to divide the $n \times n$ pixel images into $2^{cp} \times 2^{cp}$ (Anand, 2022).

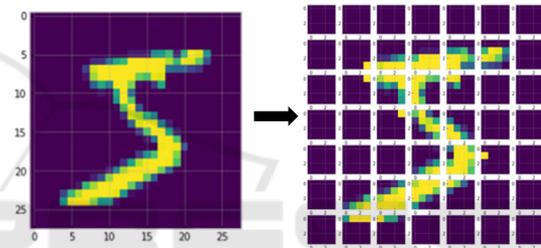


Figure 7: splitting $n \times n$ images into $2^{cp} \times 2^{cp}$.

the number of qubits here is used to design the quantum circuit of fig.7. So, suppose the pair (2, 1) N-qubits = 2 and $cp = 1$, then the appropriate chunk size is $2^{cp} = 2^1 = 2$. and so on where N-qubits are increased by 2 and cp is increased by 1 to (4,2), (6,3), (8, 4) and so on.

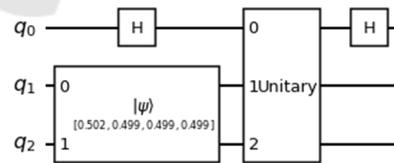


Figure 8: Example the QHED circuit with 2 qubit.

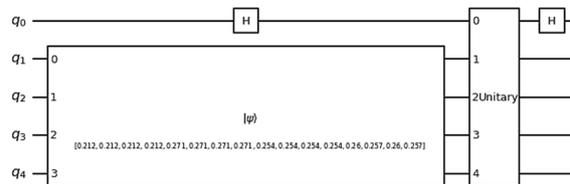


Figure 9: Example the QHED circuit with 4 qubit.

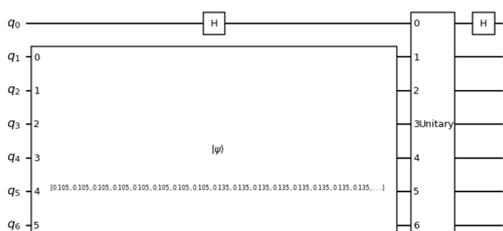


Figure 10: Example the QHED circuit with 6 qubit.

The final result of the QHED process can be seen in the following image.



Figure 11: Sample Results from the QHED.

3 EXPERIMENTAL RESULTS

A summary of test results with several image datasets used can be seen in the appendix while examples of test results can be seen in fig. 14 below.

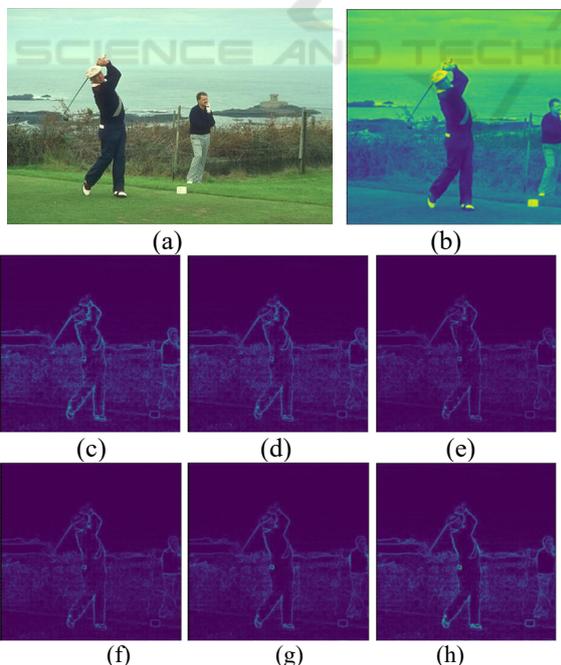


Figure 12: (a) source image (481 x 321), (b) image data (321 x 321), (c) QHED with 2 qubit, (d) QHED with 4 qubit, (e) QHED with 6 qubit, (f) QHED with 8 qubit, (g) QHED with 10 qubit, (h) QHED with 12 qubit.

From the test of some of these images, it can be seen that the highest number of segmentation in the image edge detection process is using 2 qubits.

Next, the test results of the effect of the number of qubits on CPU processing time can be seen in table 1. below.

Table 1: The number of qubits against CPU processing time (in seconds).

Image number	Number of qubits					
	2	4	6	8	10	12
1	695.68	90.16	29.25	45.76	304.59	3617.65
2	662.92	89.67	29.42	45.77	299.38	3617.10
3	795.43	103.92	33.14	49.78	361.90	5198.49
4	787.02	104.95	33.64	49.53	362.96	5183.79
5	784.99	104.34	33.44	51.20	362.05	5217.86
6	813.74	104.12	33.53	51.83	363.50	5221.86
7	756.80	99.51	32.50	48.90	362.74	5192.29
8	795.24	102.92	33.07	49.44	360.61	5221.80
9	766.54	103.11	33.26	49.31	358.62	5188.92
10	791.13	103.09	33.35	51.27	361.27	5216.15

it can be seen from table 1. Overall the fastest processing time in QHED is using 6 qubits and the longest is using 12 qubits. if we look at it as a whole, it turns out that the more the number of qubits used, the longer the processing time, but here it is found that something is different, namely the processing time using 2 qubits where the processing time is relatively longer compared to the number of qubits of 4, 6, 8 and 10. This can happen because at the QHED stage there is a process of dividing one image into several smaller image groups by splitting the images into $2^p \times 2^p$ as described in fig. 10. This study also conducted tests with 14 qubits but there was a failure in memory allocation (RAM) in this case 16 GB of RAM was unable to process all stages and data in QHED.

4 CONCLUSIONS

The results of this experiment show that theoretically QHED can perform the edge detection process in images, but from the tests carried out it was proven that the number of qubits greatly affects the CPU processing time where the fastest processing time lies in the use of the number of qubits as much as 6 qubits, not in the the least amount is 2 qubit. While the best edge detection results using 2 qubits. Then testing with a number of qubits greater than 12 qubits with 16 GB of memory (RAM) cannot be done in other words if we want to do processing with a larger number of qubits than all the stages and parameters in this study must require a larger memory (RAM) capacity as well.

ACKNOWLEDGEMENTS

This research was funded by Politeknik Negeri Bengkalis in an internal research grant (PNBP 2022) on an applied research scheme.

REFERENCES

Anand, A., Lyu, M., Baweja, P. S., & Patil, V. (2022). Quantum Image Processing. arXiv preprint arXiv:2203.01831.

Arbelaez, P., Maire, M., Fowlkes, C., & Malik, J. (2010). Contour detection and hierarchical image segmentation. IEEE transactions on pattern analysis and machine intelligence, 33(5), 898-916.

Cavalieri, G., & Maio, D. (2020). A quantum edge detection algorithm. arXiv preprint arXiv:2012.11036.

Geng, A., Moghisch, A., Redenbach, C., & Schladitz, K. (2022). A hybrid quantum image edge detector for the NISQ era. arXiv preprint arXiv:2203.12072.

Pramanik, S., Chandra, M. G., Sridhar, C. V., Kulkarni, A., Sahoo, P., DV, V. C., ... & Nambiar, M. (2021). A quantum-classical hybrid method for image classification and segmentation. arXiv preprint arXiv:2109.14431.

Ruan, Y., Xue, X., & Shen, Y. (2021). Quantum image processing: opportunities and challenges. Mathematical Problems in Engineering, 2021.

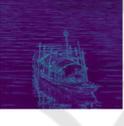
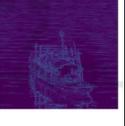
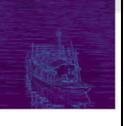
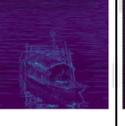
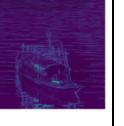
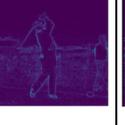
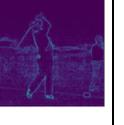
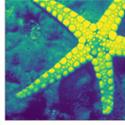
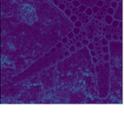
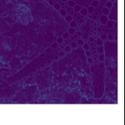
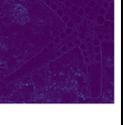
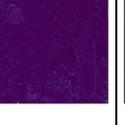
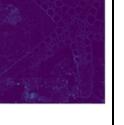
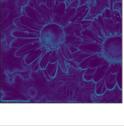
Wang, Z., Xu, M., & Zhang, Y. (2021). Review of quantum image processing. Archives of Computational Methods in Engineering, 1-25.

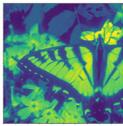
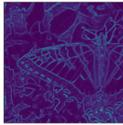
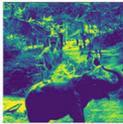
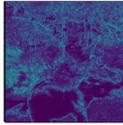
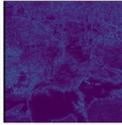
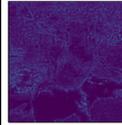
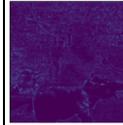
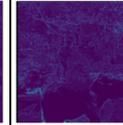
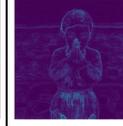
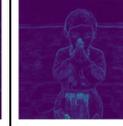
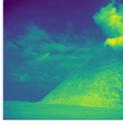
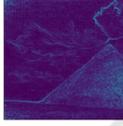
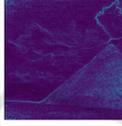
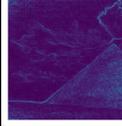
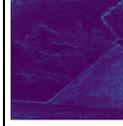
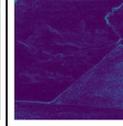
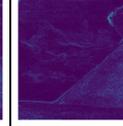
Yan, F., Iliyasa, A. M., & Venegas-Andraca, S. E. (2016). A survey of quantum image representations. Quantum Information Processing, 15(1), 1-35.

Yao, X. W., Wang, H., Liao, Z., Chen, M. C., Pan, J., Li, J., ... & Suter, D. (2017). Quantum image processing and its application to edge detection: theory and experiment. Physical Review X, 7(3), 031041.

Yuan, S., Venegas-Andraca, S. E., Wang, Y., Luo, Y., & Mao, X. (2019). Quantum image edge detection algorithm. International Journal of Theoretical Physics, 58(9), 2823-2833.

APPENDIX

No.	Source images ($w \times h$)	Images data ($n \times n$)	Number of qubits					
			2	4	6	8	10	12
1	(321 x 481) 	(321 x 321) 						
2	(481 x 321) 	(321 x 321) 						
3	(321 x 481) 	(321 x 321) 						
4	(481 x 321) 	(321 x 321) 						
5	(481 x 321) 	(321 x 321) 						

6	(481 x 321) 	(321 x 321) 						
7	(321 x 481) 	(321 x 321) 						
8	(321 x 481) 	(321 x 321) 						
9	(481 x 321) 	(321 x 321) 						
10	(321 x 481) 	(321 x 321) 					